Journal of Propulsion and Power
Vol. 26, No. 3, May–June 2010

Assessment of Seeder Performance for Particle Velocimetry in a Scramjet Combustor

J. C. Howison* and C. P. Goyne†
University of Virginia, Charlottesville, Virginia 22904

DOI: 10.2514/1.44469

The design and performance of two unique fluidized bed particle seeders were assessed experimentally. The seeders were designed to seed the fuel stream and freestream of a scramjet combustor for particle image velocimetry measurements. The fuel stream seeder used alumina powder to generate particles and has been used in the past to obtain particle image velocimetry measurements. The freestream seeder used silica powder and is a new design. Using a probe and filter paper, samples were collected from the output of each seeder at operating conditions near those encountered in scramjet particle image velocimetry studies. The samples were imaged using a scanning electron microscope to obtain qualitative and quantitative data about the particles generated. Both seeders produced particles near the target size of 0.3 μm, although the silica particles were generally smaller in size and more spherical than the alumina particles. Based on these results, it was predicted that the freestream particles would scatter light more uniformly and track the flow more faithfully than the fuel stream particles. The results of this study confirm assumptions on particle size and shape made in previous particle image velocimetry experiments and also indicate that the fuel stream seeder will generate more effective particles using silica powder.

Nomenclature

A_P	=	area of particle
a	=	speed of sound
C	=	characteristic frequency of the particle motion
C_D	=	drag coefficient
d_P	=	particle diameter
$\mathrm{d}V_p/\mathrm{d}t$	=	particle acceleration
F	=	shearing force on particle
M	=	Mach number
Re	=	Reynolds number
$\bar{u}_f^2$	=	fluid velocity fluctuations
$\bar{u}_p^2$	=	particle velocity fluctuations
V_g	=	gas velocity
V_p	=	particle velocity
μ	=	viscosity
ρ_g	=	density of the gas
ρ_p	=	density of the particle
ω_c	=	angular frequency of turbulent motion

Introduction

PARTICLE image velocimetry (PIV) has become a common nonintrusive method that is used by experimentalists to investigate many different types of flows, including subsonic, supersonic, mixing, and combusting flows. A key advantage of the application of PIV to high-speed flows is that measurements can be taken without the flow being disturbed by the presence of probes [1,2]. However, the technique relies upon using a suitable seeding concentration with appropriately sized, monodisperse particles to produce quality results. Proper particle size is necessary so that the particles are large enough to provide a strong signal-to-noise ratio for the particle imaging technique, but also small enough to faithfully track the flow. Uniform seeding size helps avoid excessive intensity from larger particles and background noise from smaller particles [3].

Extensive literature exists for different methods of particle seeding [3–5]. Condensation and atomization are the most common for liquid droplets, whereas atomization and fluidized beds are the most common for solid particles. Atomizers can disperse solid particles in an evaporating liquid or create high-vapor-pressure droplets in a low-vapor-pressure gas. In a fluidized bed, particles are suspended in a chamber and then drawn out of the top for dispersion into a flow. Fog machines may also be used to seed gas flows by dispersing condensed oil droplets throughout the flow. There are a variety of particle types as well. Some of the more common particles used in gas flows include oil droplets, polystyrene, titanium dioxide (TiO_2), alumina (Al_2O_3), and silica (SiO_2). For high-temperature flows, the particles must have a sufficiently high melting or boiling temperature to scatter light and not break down.

The present study is concerned with the application of PIV to a scramjet combustor in a supersonic combustion facility, in which high temperatures and velocities make most seeding methods unfeasible. This facility produces a Mach 2 flow using heated air [6,7]. The supersonic combustion of hydrogen in a scramjet is studied using a single 10 deg unswept ramp fuel injector. Temperatures in the combustion chamber approach 1200 K during mixing and 2400 K during combustion. Successfully seeding such a flow is challenging. To obtain velocity information on the entire combusting flowfield using PIV, both the fuel stream and freestream must be seeded with particles. This is especially important in the region near the fuel injector. Particles injected into the fuel stream cannot be used to provide velocity data on the freestream until the two streams have sufficiently mixed and vice versa. Because velocity data in the mixing region are of high interest in combustion problems, it is necessary to effectively seed both streams to gather PIV data throughout the entire combustor. Although the fuel stream has been successfully seeded for PIV [1,8], no data have obtained from seeding the freestream because an effective seeder has yet to be implemented. The freestream has a flow rate approximately 250 times that of the fuel stream, which, as will be discussed in this paper, dictated that the freestream seeder have a modified design from the fuel stream seeder.

This paper presents the unique designs of the fuel stream and freestream seeders created to study supersonic combustion within a scramjet engine using PIV. Individual seeder performance is usually assessed in high-speed PIV by assuming an output particle size from the size specifications of an input seeding material. Because particles have a tendency to agglomerate, this leads to incorrect assumptions

Received 20 March 2009; revision received 10 February 2010; accepted for publication 22 February 2010.

*Graduate Research Assistant, Aerospace Research Laboratory, Post Office Box 400248. Student Member AIAA.

†Research Assistant Professor, Department of Mechanical and Aerospace Engineering, Post Office Box 400746. Associate Fellow AIAA.

on the light scattering and flow tracking behaviors of the particles, which leads to errors in assessing the accuracy of PIV data. This work will show the results of experiments conducted to directly measure the output particle size by a fuel stream and freestream seeder. In the experiments, particles were sampled from seeded airflows using a probe and filter paper. The particle size and shape were determined directly by analyzing images from a scanning electron microscope (SEM) of the particles on the filter paper. These results will be presented along with a discussion on the theoretical light scattering and flow tracking ability of the particles' output by each seeder. These results make it possible to quantify the experimental uncertainty associated with the particles from these seeders in PIV measurements.

Experimental Approach

Based on previous PIV experiments, a fuel stream seeder using alumina powder in a fluidized bed and a freestream seeder using silica powder in a fluidized bed were chosen for implementation. Alumina powder was chosen for the fuel stream seeder because of its ability to withstand high temperatures and its relatively low cost. The drawback of the alumina powder was the nonuniform, jagged shape of the primary particles, which promoted particle agglomeration. However, a shearing nozzle near the exit of the fuel stream seeder was found to be effective at breaking down these agglomerates. This nozzle worked by injecting the particles transversely into a high-speed flow. Preliminary tests of the alumina powder within the freestream seeder indicated sufficiently small particles could not be produced. A powder composed of primary particles less prone to agglomeration was desirable for the freestream seeder because the higher flow rate of the freestream precluded the use of a shearing nozzle. Silica powder was hence chosen for the seeder despite its higher cost because its primary particles were more uniform and nearly spherical in shape and also because of its ability to withstand high temperatures. It was anticipated that the spherical shape of the silica particles would reduce the ability of particles to agglomerate.

In addition to shape, the choice of particle size is a critical decision in PIV implementation. The choice of optimal diameter for seeding particles is a compromise between an adequate response of the particles to changes in the flow velocity, requiring smaller diameters, and a high signal-to-noise ratio of the scattered light signal, necessitating larger diameters [3]. There is a limit, however, on the accuracy of PIV measurements due to particle lag error, which can be determined by examining the ratio of the particle response time to the flow time scales [9]. Previous work by Goyne et al. [10] indicated that 0.3-μm-diam sized particles are a suitable balance between flow tracking and light scattering ability for the PIV applications of interest. Even though the alumina and silica powders have particle diameters specified by their manufacturers at 0.3 and 0.25 μm, respectively, it cannot be assumed that the seeders are producing particles of these sizes. For example, Ross et al. [11] found that their PIV seeding system produced particles with an average diameter of 0.9 from 0.3 μm nominal particles while measuring a supersonic flow past a 2-D wedge. As mentioned earlier, this is because particles tend to agglomerate, especially after periods of storage or exposure to humidity. Thus, it was necessary to assess the performance of each system by measuring the output particle size.

Several possibilities were considered for examining the sizes of the particles' output by the seeders. PIV images have been used by others to measure particle sizes [12], but a high level of accuracy at the submicron level with this method is extremely difficult to achieve. Alternatively, a laser can be used to observe a particle's diffraction or its aerodynamic flight time [13]. The former method, particle diffraction, correlates the intensity and angle of light scattered by particles to their sizes. The latter method, particle aerodynamic flight time, looks at the deceleration of a particle between two light sources and then determines particle size using the known density of the particle material. However, nonagglomerated particles are preferred for both methods to minimize error, and one of the reasons for the present study is to determine if the particles are agglomerated or not. It was decided that directly determining particle size from images of samples collected from seeded flows with a scanning electron microscope (SEM) would be the most reliable and easily implemented method. This method would also allow for the observation of the particles' shapes, which would not be possible with any of the other methods. Knowledge of the particles' shapes is significant because this work also seeks to predict the light scattering and flow tracking abilities of the particles. The accuracy of these predictions can be gauged even with a qualitative understanding of the particles' shapes because both prediction models assume a spherical shape. The details of each seeder's design and how each design meets established design criteria will first be examined in the following section.

Seeder Design

Because of different operating conditions, the fuel stream and freestream seeders required different designs. Each seeder was designed with four main criteria: 1) output particle size and particle size distribution, 2) output particle number density, 3) operating pressure and pressure drop, and 4) controllability. The first point emphasized the need to design a seeder that produced particles near 0.3 μm in size as required by the PIV experiments. The number density was critical because at least 10 particle image pairs are recommended per PIV interrogation region [14]. However, the density could not be too high either as that could lead to difficulty in distinguishing individual particles in PIV data processing. The seeders also needed to operate at pressures higher than the flow in which the particles would be injected, but the operating pressure was to be minimized above that point so as to reduce pressure vessel design requirements. Likewise, pressure drops in the seeders were to be minimized because a larger pressure drop would require a higher supply pressure. Finally, the seeders needed to have controllability over the output number density so that the seeding could be adjusted as necessary during PIV experiments.

Both seeders were designed using a simple fluidized bed approach in which a gas enters a chamber through a porous material to create a slow, uniform flow. The drag force on the particles in the chamber created by the uniform flow is just large enough to overcome the opposing gravitational force. This suspends the particles to create an aerosol, which is then drawn out of the chamber for dispersion into the flow. Small modifications were made to each design to assist in breaking down agglomerates of particles. The fuel stream seeder design will now be presented, followed by the freestream seeder design.

Fuel Stream Seeder

The fuel stream seeder is shown in Fig. 1. This seeder has been previously used for PIV measurements in a hydrogen-fueled scramjet [1,8]. The seeder used a fluidized bed along with a fine pickup tube and shearing nozzle. Most of the hydrogen flow went along path A, where it was accelerated to Mach 3 in a shearing nozzle and then shocked back to subsonic prior to the fuel being injected into the scramjet. Some of the remaining flow went along path B to be used in the fluidizer. The fine pickup tube fed the fluidized particles to the shearing nozzle, at which point the particles were injected transversely into the flow at a location where the flow had reached Mach 2. The high-speed flow created by the supersonic nozzle effectively sheared apart any agglomerates. This method of shearing agglomerates is based on a concept employed by Smith [15]. A remotely operated metering valve controlled the flow rate through the fluidizer, which, in turn, controlled the seeding rate. The total pressure at the outlet of the seeder was adjusted by adjusting the flow rate along path C. Further information on the seeder is available [10,16].

Alumina (Al_2O_3) powder was chosen to seed the fuel stream based on previous PIV studies of high-speed combusting flows. The manufacturer's specified nominal particle size was 0.3 μm with a particle density of 3940 kg/m^3. The nominal agglomerate size during storage was measured to be between 2 and 40 μm. The particles had melting and boiling points of 2400 and 3300 K, respectively, so particle breakdown was not expected when tracking the hydrogen–air combusting flow, which reaches a maximum

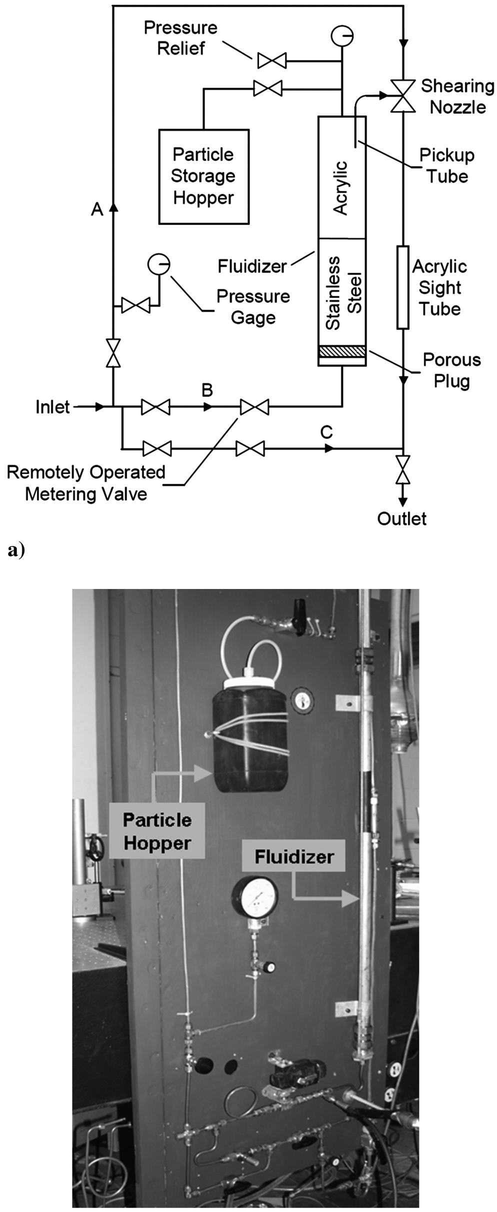

a) b)

Fig. 1 Fuel stream seeder apparatus: a) schematic and b) picture.

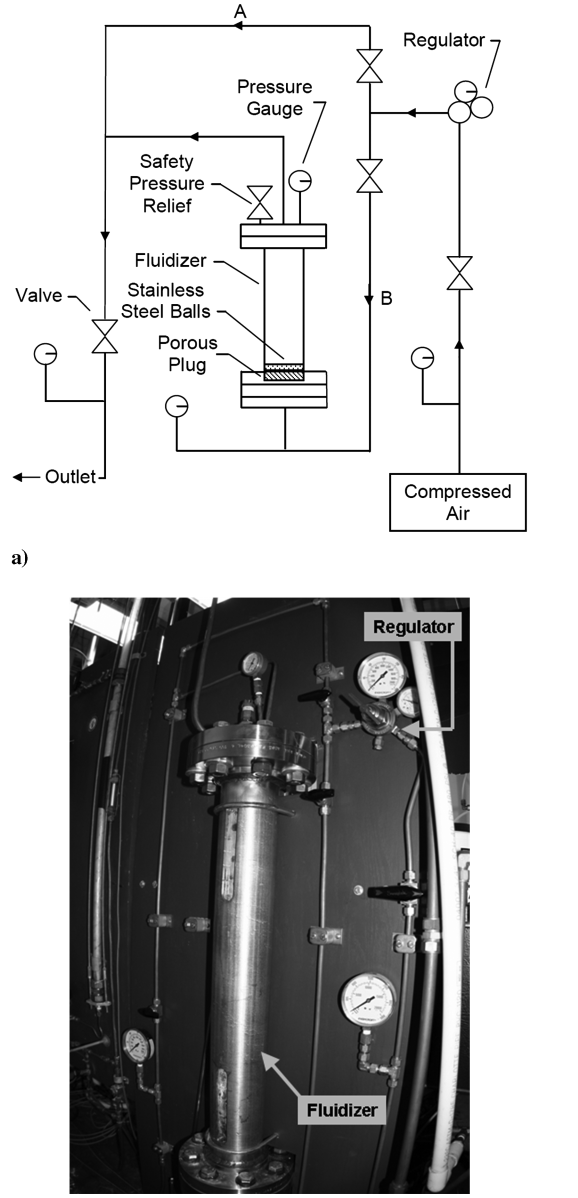

a) b)

Fig. 2 Freestream seeder apparatus: a) schematic and b) picture.

temperature of approximately 2400 K. This design required an operating pressure of up to 700 kPa in the fluidizer, which was easily accommodated by the high-pressure hydrogen supply. Moreover, controllability of the seeding density was met by the adjustability of the flow through path B.

Freestream Seeder

The freestream seeder design was essentially the same as the fuel stream seeder design with the exception of the shearing nozzle and operating gas. A particle shearing nozzle could not be used for the freestream seeder because the facility air compressor could not provide a large enough pressure difference above the wind-tunnel operating pressure to run a supersonic shearing nozzle. Particles with a lower tendency to agglomerate were sought for the freestream seeder for this reason. The freestream seeder design also employed a fluidized bed and is presented in Fig. 2. The flow of air was split, with path A bypassing the fluidizer and path B going to the fluidizer. Once particles rose to the top of the fluidizer, they flowed to the exit of the seeder for injection into the flow. Because the porous plug was not sufficient in creating a completely uniform flow in the fluidizer, an approximately 1.5-cm-thick layer of stainless steel balls (3.2 mm in diameter) was added to the bottom of the fluidizing chamber to assist in creating a more uniform flow.

Amorphous silica microspheres with a manufacturer-specified diameter of 0.25 ± 0.05 μm and particle density of 2000 kg/m^3 were chosen as seeding particles. Although no melting or boiling point is specified by the manufacturer, silica's melting and boiling points are over 1800 and 2500 K [17]. Given the maximum expected temperature of 2400 K in the scramjet, the particles may melt, but they will not boil and vaporize. Therefore, particle breakdown during combustion testing is not expected. The seeder was designed to operate at 410 kPa with little or no pressure drop, which was well within the pressure vessel design criteria. Additionally, the seeding density could be controlled by adjusting the seeder's supply pressure or by changing the amount of flow between paths A and B. Because control of the seeding density was not necessary in this experiment, path A was closed and all of the flow was allowed to enter the fluidizer.

Experimental Technique

For both seeders, the output seeded flow was sampled using a probe and filter paper coupled to a vacuum pump. The particles could not be sampled from the fuel stream or freestream at actual scramjet wind-tunnel conditions due to the high temperatures and velocities involved. Therefore, experiments were designed for collecting samples from each seeder that allowed for the operation of each at typical experimental conditions. In both cases, a flow was seeded that was similar to that of an actual combustion experiment, and then particles were sampled from that flow. In the case of the fuel seeder, the stagnation pressure upstream of the fuel injector nozzle was matched, which ensured that the shearing nozzle was fully started. For the freestream seeder, the velocity and cross-sectional area at the point of particle injection into the freestream were matched so that particles mixed into the flow and were sampled from a volume representative of a combustion experiment. The fluidizers were operated at the same pressure differentials as used during normal operation.

Isokinetic sampling is accomplished if the flow rate in a gas freestream matches the flow rate of the gas entering a sampling probe. Sampling in this way guarantees that particles of all sizes have an equal probability of being collected because the streamlines in the probe and freestream remain parallel. Too low a flow rate inside the probe will cause streamlines to diverge away from the probe, which biases the sample toward larger particles because their higher inertia makes following the diverged streamlines difficult. The opposite will happen if the flow rate inside the probe is too high, and the streamlines converge into the probe [18]. Because of limitations in the experimental equipment, all the samples were collected at less than isokinetic flow rates. This gave a bias toward larger particles so that conservative results were obtained for a particle size that is sufficiently small for PIV. In other words, the size of the particles actually sampled may be somewhat larger than the particles in the seeded flow. Therefore, if the results of the present study are used to assess flow tracking, the particles in the seeded flow will actually perform better than predicted. The details of the fuel stream seeder experiment are now examined, followed by details of the freestream seeder experiment.

Fuel Stream Seeder

An overview of the experimental setup for the fuel stream seeder is presented in Fig. 3. The experiment was originally reported in [19]. Seeded flow exited the fuel stream seeder and entered an exhaust nozzle. The exhaust nozzle was added to the flowpath after the outlet of the particle seeder for the purpose of matching the throat diameter to that of the fuel injector used by the supersonic combustion facility. This kept the stagnation pressure upstream of the exhaust nozzle close to the fuel injector's operating stagnation pressure because the gas supply pressures were the same. This ensured that the experiment accurately modeled the particle shearing and dispersal behavior present in PIV experiments. A sampling probe was mounted to a traverse, enabling the probe to be moved throughout the flow. A vacuum pump controlled the pressure differential on the system and kept the seeded flow moving through the sampling probe and over a filter paper. This prevented stagnation at the probe inlet. A more detailed description of the setup is available in [19].

A 1.32-mm-diam sampling probe was constructed out of Inconel tubing. The probe diameter was specified such that the maximum allowable flow rate through the filter paper would not be exceeded. The outer walls of the probe inlet were designed to include a 20 deg sharp leading edge so as to prevent a bow shock from creating spillage at the probe inlet. The probe was placed 64 mm downstream of the exhaust nozzle, slightly off the jet centerline. The filter paper was a 0.1 μm mesh made from a cellulose nitrate membrane, 47 mm in diameter. Mesh size is used to describe the diameter of the pores in the filter paper, and particles larger than the mesh are trapped on the surface of the filter paper. The filter holder was designed in such a way so as to allow particles to be captured over the entire surface. The paper was rated at a volumetric flow rate of 0.67 $\mathrm{L/min/cm^2}$.

Nitrogen and helium were used as the seeded gas. Although the seeder is ultimately designed for use with hydrogen, it was impractical and hazardous for this experiment. Because the particle size will primarily be determined by the strength of the shear force in the shearing nozzle, which as discussed later is proportional to the product of gas viscosity and velocity within the nozzle, the results can be extrapolated to hydrogen. The total pressure of the gas upstream of the seeder was 20 bar, which resulted in a total pressure downstream of the seeder of 10 bar with a pressure ratio across the exhaust nozzle of 10. The seeder gas total temperature was at 300 K throughout the experiment. The ratio of the mass flux of seeded flow to the mass flux in the sampling probe needed to be unity for isokinetic sampling. Of the two gases used to seed the particles, the ratio for nitrogen was 6.0 and the ratio for helium was 4.5 [20]. This created the aforementioned bias toward larger particles because the flow rate inside the probe was less than that of the freestream.

To image samples using the SEM, each filter paper was cut in half with one half being mounted for use in the SEM. Samples were set on aluminum mounts using electrically conductive two-sided tape and imaged at magnifications ranging from 2000x to 50,000x.

Freestream Seeder

The freestream seeder was tested using a room temperature flow of air through an acrylic tube. A blower was used to create a flow that was similar in velocity to the flow encountered at the point of injection in the scramjet combustion facility (21 m/s in the acrylic tube compared with 16 m/s in the combustion facility). The higher pressure encountered in the combustion facility, 0.3 MPa compared to 0.1 MPa in the blower, was not considered a problem because drag, a function of viscosity and velocity, is the dominant factor in shearing apart the agglomerates. An overview of the setup is given in Fig. 4. The particle-laden air from the seeder was injected against the flow direction using the actual wind-tunnel freestream injector. This injector consisted of a 34.9 cm metal rod with a single injection hole at one end. Particles are also injected against the flow in the wind-tunnel experiments to promote particle deagglomeration through increased drag forces. The same sampling probe from the fuel stream experiments was used and placed approximately 32 mm downstream of the injector. The air was sampled at a rate 4.4 times less than isokinetic. A vacuum pump maintained airflow through 0.1 μm filter paper with a rotameter and vacuum gauge connected to verify flow conditions.

The freestream seeder was designed to operate using dry air bled off of the wind-tunnel compressor during supersonic combustion

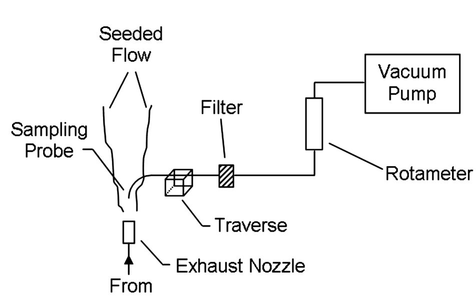

Fig. 3 Overview of fuel stream seeder experimental setup.

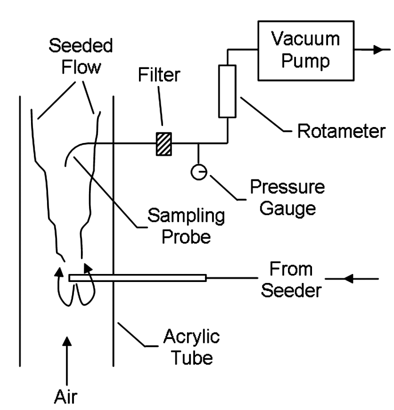

Fig. 4 Overview of freestream seeder experimental setup.

experiments. For this experiment, nitrogen was a convenient, comparable alternative with 78% of air being composed of nitrogen by volume. The static pressure of the fluidizer was also changed from normal wind-tunnel operating conditions to keep the pressure difference across the fluidizer at a typical PIV experimental value of 70 kPa, because it is this pressure difference that drives the fluidizing process. Preliminary work seeding the freestream indicated that a 70 kPa pressure difference provided the required particle seeding density for PIV imaging. The conditions of both experiments are summarized in Table 1.

SEM samples were mounted and coated with a 10–20 nm layer of gold palladium to reduce image drifting under high magnification due to a charge buildup. This buildup occurred because SEMs use beams of electrons to create an image of the sample, and the particles and filter paper were both nonconductive. No coating was necessary with the alumina samples from the fuel stream seeder because of the decreased resistivity of alumina. Magnifications ranged from 3000x to 30,000x.

Image Processing

The nonhomogeneous nature of the filter paper made it difficult for computer software to discern between particles and filter paper. As a result, Owens et al. [19] found that developing an automated process that could extract quantitative data from the SEM images was very challenging. Manual inspection proved to be an easier technique for image processing. The particles' characteristic lengths were measured using image-viewer software, in which a particle's longest linear dimension was defined as its characteristic length. This was the simplest and most conservative method of applying a metric for comparing particles of differing sizes and shapes. The method is conservative toward small particles because the characteristic length will be assumed to represent the particle diameter, and oblong particles, for example, will have larger diameters than their true effective diameters under this method. The characteristic length was measured in pixels and then converted to metric units using a reference scale included on the SEM images. The application of this technique to each seeder's particles will now be discussed.

Fuel Stream Seeder

The fuel stream seeder particles varied in size by nearly three orders of magnitude. As a result, images were analyzed at three different magnifications using a method developed in [19] so that particles of all sizes could easily be counted and resolved. Figure 5 illustrates this method. Care was taken not to count and measure the same particle at two different magnifications to eliminate any overlapping of data. By assuming an even distribution of particle sizes over the filter paper, the results from higher magnifications could be extrapolated to the area from lower magnifications. For example, the results from an image with a 10 times higher magnification were multiplied by 10 to scale them up to the results from the lower magnification image. It is noted that this method gives considerable weighting to the highest magnification, and so extreme caution was used in counting and measurement at this level. The method was validated in [19] by comparing results from the same-sized particles examined at two different magnifications with satisfactory agreement being found.

Freestream Seeder

Images produced from this experiment were much easier to work with because the particles were all of the same order of magnitude

Table 1 Test conditions

Parameter	Fuel stream seeder	Fuel stream seeder	Freestream seeder
Seeder gas	He	N_2	N_2
Powder type	0.3 μm Al_2O_3	0.3 μm Al_2O_3	0.25 μm SiO_2
Primary filter paper	0.1 μm	0.1 μm	0.1 μm

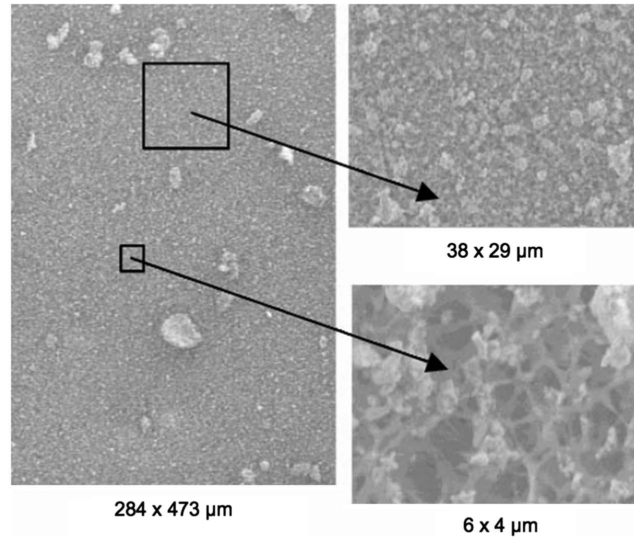

Fig. 5 Image processing methodology for fuel stream seeder. Image boxes are not drawn to scale (reproduced from [19]).

and contrasted better with the filter paper background. Therefore, the results presented here were obtained from the same magnification, 3000x. However, the analysis was also conducted at 10,000x to check for consistency, with the sample means differing by only 0.03 μm. This was within the manufacturer-specified particle size tolerance of ± 0.05 μm.

Results and Discussion

Several of the properties of the particles from each seeder are presented in this section. First, particle shape and size are discussed as obtained from direct analysis of the SEM images. A qualitative knowledge of the particle shape helps assess the uniformity of the particles and determine the validity of assumptions of spherical particles in light scattering and flow tracking analyses. Particle size is critical because 0.3-μm-diam particles are most desirable for the supersonic combustion PIV work described earlier. The particles' abilities to scatter light and accurately track high-speed and turbulent flows are examined next. As discussed earlier, uniform light scattering from all particles in the flow is key to obtaining PIV data with a strong signal-to-noise ratio. Accurate flow tracking of high-speed structures and turbulence by the particles is also critical in obtaining quality PIV data because the PIV method is based on seeder particles effectively tracking structures within a flow.

Particle Shape

Using the SEM to create images of samples enabled a close-up look at the shape of sampled particles. Figure 6 shows particles from the fuel stream and freestream seeders at 5000x and 3000x, respectively. As can be seen in the figure, the silica particles from the freestream seeder were nearly spherical, whereas the alumina particles from the fuel stream seeder were rounded, irregular, or ligamental. Later analyses of light scattering and flow tracking behavior will assume a spherical shape for all particles based on the characteristic length representing the diameter. This assumption is clearly valid for primary silica particles, but more approximate when applied to agglomerated silica particles and both primary and agglomerated alumina particles, as evidenced in Fig. 6.

Particle Size

Histograms for the particle sizes from each of the three cases, helium and nitrogen in the fuel stream seeder and nitrogen in the freestream seeder, are reported in Fig. 7. The histogram for the fuel stream seeder was truncated at 1 μm, whereas that of the freestream seeder was truncated at 0.5 μm because the remaining particles were

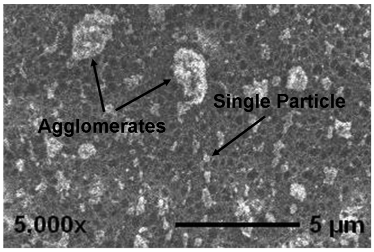

a)

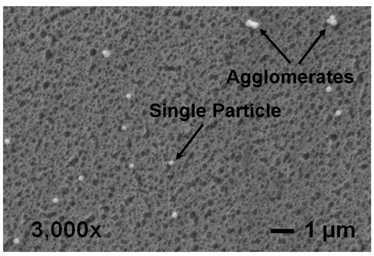

b)

Fig. 6 SEM image of particles on filter paper from the seeder: a) fuel stream, and b) freestream.

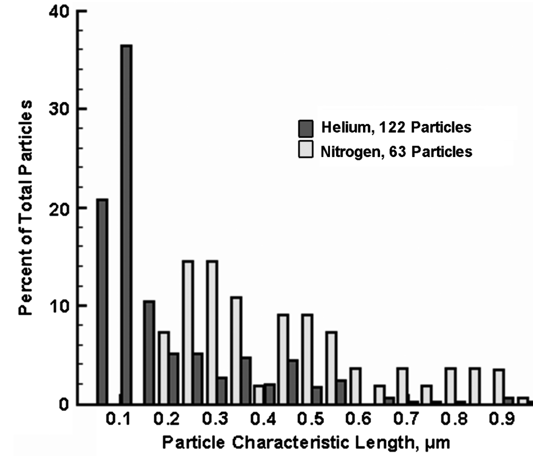

a)

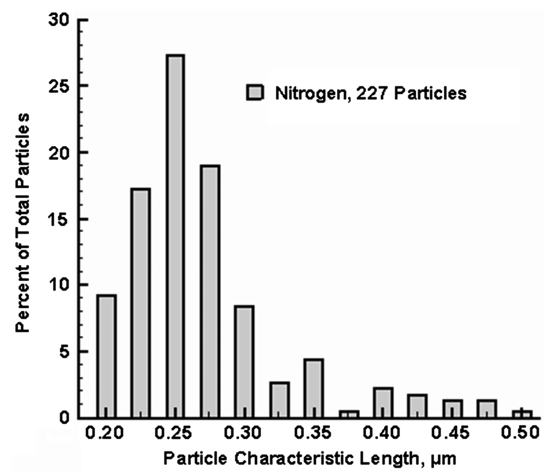

b)

Fig. 7 Histogram of particle sizes for the seeder: a) fuel stream and b) freestream.

only a few percent of the total particle count (for the fuel stream seeder with helium, 1.5%; with nitrogren, 3.0%; and for the freestream seeder, 4.4%). The data shown for the fuel stream seeder operating with nitrogen are from 63 particle measurements from two separate images. When operating with helium, the fuel stream seeder data are based on 122 particles measured from three separate images. Finally, the freestream seeder's data come from 227 measured particles in four separate images. The uncertainty in the particle size measurements was calculated as the root mean square of the sum of the precision error in the data, the resolution of the images, and the operator error. The precision error was calculated using a 95% confidence interval and assuming a student's t-distribution. In all cases, it was assumed that the operator error in defining the characteristic length was ± 2 pixels.

All of the graphs in Fig. 7 exhibit a lognormal distribution, which is expected from naturally occurring particle aggregates [21]. Examination of Fig. 7a reveals that helium created smaller particles than did nitrogen in the fuel stream seeder. This is a result of a higher viscosity and velocity in the shearing nozzle of helium over nitrogen. This creates larger shearing forces within the shearing nozzle, which, in turn, produces smaller seeding particles through deagglomeration. The shearing mechanism is further discussed later. The mean particle size for helium was $0.23 \pm 0.03\ \mu$m and for nitrogen was $0.49 \pm 0.1\ \mu$m, which is consistent with this explanation. The freestream seeder's output, shown in Fig. 7b, lies between the two cases studied in the fuel stream seeder with an average seeder output particle size of $0.27 \pm 0.07\ \mu$m. The uncertainty for the freestream seeder output is close to the manufacturer-specified tolerance of $\pm 0.05\ \mu$m. It is interesting to note that 198 of the 227 particles counted were composed of only a single primary silica particle, and most of the remaining particles were composed of two primary particles stuck together. This is significantly less agglomeration than seen from the alumina particles in the fuel stream seeder. This means that the seeder is effectively breaking down agglomerates and/or the particles do not form a large proportion of agglomerates in the first place. The results are summarized in Table 2.

Cumulative distributions of the particle sizes from each of the cases are shown in Fig. 8. Inspection reveals that approximately 80% of alumina particles from the fuel stream seeder operating with helium and 80% of silica particles from the freestream seeder were smaller than the target particle size of 0.3 μm. Only 20% of alumina particles from the fuel stream seeder operating with nitrogen were smaller than the target size. The differences in size between the two fuel stream seeder cases are to be expected given the greater shearing force that is created when helium is used as the seeding gas. The matching trends of the fuel stream seeder with helium and the freestream seeder are encouraging for potential future PIV tests. It suggests that both seeders are capable of producing similar particle size distributions close to the target size. However, it must be recognized that neither experiment used the seeding gases that are used during PIV combustion tests, that is, hydrogen and air. In what follows, the results are extrapolated to these different gases so that effects on particle size may be examined.

Starting first with the fuel seeder, particle agglomerates are broken down in the shearing nozzle via a shear force that results from particle drag. This force can be calculated from the definition of the drag coefficient for a particle, $C_D = F/\frac{1}{2}\rho_g V_g A_p$. The drag coefficient can be estimated via Stokes' drag [3], $C_D = 24/Re$ (to simplify the analysis, the modified Stokes' drag approach that is used later is not adopted here). From knowledge of the drag coefficient, the shearing force can be shown to be linearly proportional to the product of the viscosity and velocity of the gas at the point of agglomerate injection into the shearing nozzle. For the supersonic shearing nozzle, this product is approximately equal to the product of gas viscosity and

Table 2 Summary of results

Seeder	Avg. size	Count	Error
Fuel stream, He	0.23 μm	63	$\pm 0.03\ \mu$m
Fuel stream, N_2	0.49 μm	122	$\pm 0.1\ \mu$m
Freestream, N_2	0.27 μm	227	$\pm 0.07\ \mu$m

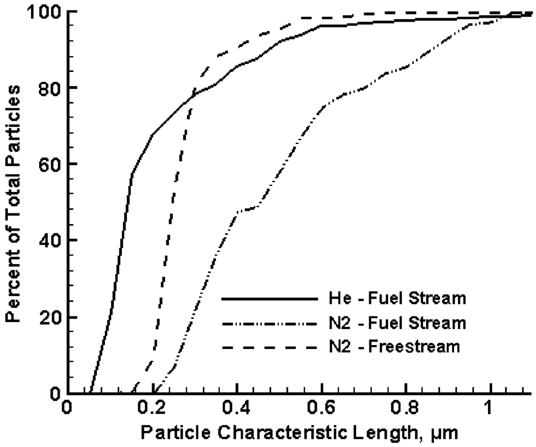

Fig. 8 Cumulative particle size distribution.

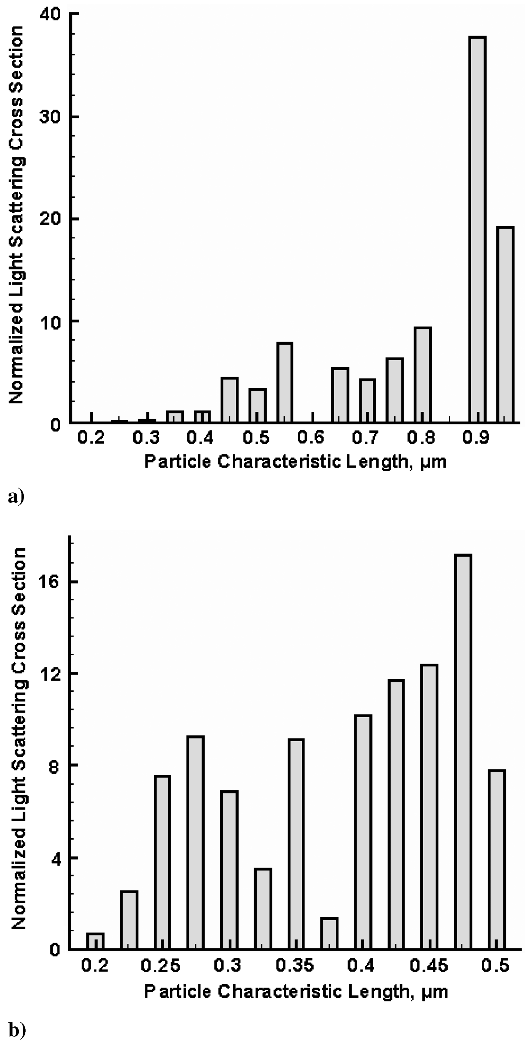

Fig. 9 Normalized Mie light scattering cross section for the seeder: a) fuel stream, and b) freestream.

speed of sound, which, when normalized by the value for air, is 0.98 for nitrogen, 1.9 for hydrogen, and 2.1 for helium. This means that the shearing force on agglomerates for hydrogen and, hence, the resulting particle size will be somewhere between that of nitrogen and helium, and will be closer to that of helium. Reference to Table 2 and a linear interpolation of the product of gas viscosity and speed of sound yields a predicted mean particle size of 0.28 μm for hydrogen.

For the freestream seeder, the viscosity and speed of sound of the seeded gas is not expected to have any effect on the average particle size because the gas is only acting as a fluidizing medium, because the freestream seeder does not operate with a shearing nozzle. Therefore, an equal particle size is expected in the freestream seeder regardless of the seeded gas type.

Light Scattering

For particle imaging techniques, the light scattering ability of a particle is critical to its effectiveness at providing useful knowledge of the flow. Too large a particle will saturate light sensing equipment, whereas too small a particle will only generate noise. The theoretical light scattering cross section was calculated for the measured particle sizes from the fuel stream and freestream seeders using the approach taken in [19]. Only the helium case is used from the fuel stream seeder because those results best reflect the expected performance of the seeder when operating with hydrogen.

It was assumed that the particles will scatter light according to Mie theory because the particle characteristic lengths were of the same order of magnitude as the wavelength of typical PIV lasers, 0.532 μm. It was also assumed that the scattering cross section scaled to the particle characteristic length raised to the sixth power [22]. The observation angle, also sensitive to the particle size, was neglected because the camera placement will vary across different PIV experiments. Figure 9, showing the light scattering cross sections as a function of particle size, was produced using the size distributions shown in Fig. 7.

Because Mie theory applies to spherical particles, the results for the fuel stream seeder are approximate, whereas those for the freestream seeder are more realistic given the shapes observed in Fig. 6. However, this analysis seeks to provide only a qualitative assessment of the different particles' abilities in light scattering. It is clear in Fig. 9 that the larger alumina particles dominate the scattering from the fuel stream seeder particles, whereas a range of silica particles from the freestream seeder scatter comparable quantities of light. The signal produced by the freestream particles will be superior to that of the fuel stream particles because large particles will not drown out the signal from smaller particles. The fuel stream particles will actually scatter light more uniformly than seen in Fig. 9 during PIV experiments because the use of hydrogen in the seeder will decrease the population of large agglomerate particles through larger shearing forces. Nevertheless, the use of silica powder in the fuel stream seeder is advisable for the future in terms of light scattering because the uniform spherical shape of the primary particles lends itself to a more uniform light scattering and, thus, better signal-to-noise ratio in the data.

Flow Tracking

The accuracy of PIV results is strongly influenced by the seeding particles' abilities to faithfully track velocity gradients within a flow. A theoretical calculation of the relaxation distance after crossing a shock wave is a common method for quantifying a particle's ability. Flow across an oblique shock wave is considered here to investigate each particle's flow tracking ability using the approach taken in [19]. Because the step change in velocity across a shock is nearly instantaneous, studying a particle's ability to track such a change is a convenient way to measure its flow tracking ability across a large disturbance. The case considered is depicted in Fig. 10, in which an oblique shock is generated in a Mach 2 airflow with a velocity of $V_1 = 1060$ m/s over a 10 deg wedge. These conditions were chosen as they are typical of the conditions seen in [1,8]. The velocity vectors V_1 and V_2 shown in Fig. 10 correspond to the streamline velocities upstream and downstream of the shock, respectively, and V_{1n} and V_{2n} are the velocity components normal to the shock.

Meyers's modified Stoke's drag approach in [4] was used to calculate the particle acceleration after the oblique shock. Because the particle density is much greater than that of the fluid, the particle motion can be adequately described using only Stokes' drag as the force term. The particle acceleration can then be described by

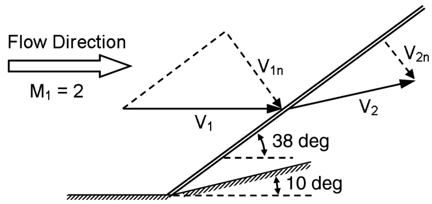

Fig. 10 Oblique shock formation on a 10 deg wedge.

$$\frac{\mathrm{d}V_p}{\mathrm{d}t} = \frac{3}{4}\frac{C_D \mu Re}{\rho_p d_p^2}(V_g - V_p) \tag{1}$$

The model presented assumes spherical particles. This assumption applies to the primary silica particles, but is more of an approximation for the alumina particles and agglomerates of both, as stated earlier. The input parameters for the analysis are summarized in Table 3. By applying this particle drag model to the particle distributions shown in Fig. 8, it was possible to determine the proportion of particles accurately tracking the flow at a given normal distance downstream of the shock. Again, only the helium case is used from the fuel stream seeder because those results best reflect the expected performance of the seeder when operating with hydrogen. It is noted for clarification that the analysis used the properties of air because the flowfields to be studied using these seeders are composed of mostly air.

A particle was considered to be effectively tracking the flow if its velocity was within 10% of the fluid velocity. Figure 11 shows the proportion of particles tracking the flow as a function of the normal distance downstream of the shock. Nearly 90% of the freestream particles are tracking the flow 2 mm downstream of the shock, whereas only 70% of the fuel stream particles are tracking the flow at this point. Approximately 100% of the freestream particles are tracking the flow around 3.8 mm downstream of the shock, at which point approximately 90% of the fuel stream particles are tracking the flow. This demonstrates that the particle lag will be less for particles produced by the freestream seeder across discontinuities.

A particle's response to turbulence was also considered. PIV results are only capable of showing the turbulent structures in a flow if the particles are able to adequately track the turbulent motions. The approach taken by Melling [3] is used here. A particle was considered to be responding to turbulence in the flow if the ratio of the fluctuation intensities of the particle and fluid motion, the left-hand side of Eq. (2), was equal to 0.95:

$$\bar{u_p^2}/\bar{u_f^2} = (1 + \omega_c/C)^{-1} \tag{2}$$

where

$$C = 18\mu/\rho_p d_p^2 \tag{3}$$

The plot in Fig. 12 shows the percentage of particles responding to a given turbulence frequency in the flow. All the freestream particles are capable of responding to turbulence frequencies less than 10^3 Hz, and 95% of them will respond to frequencies less than 10^4 Hz. Nearly all of the fuel stream particles will also respond to turbulence frequencies less than 10^3 Hz, but only around 80% will respond to

Table 3 Flow tracking calculation parameters

Parameter	Value
V_{n1}, m/s	656
V_{n2},m/s	447
Gas density behind shock, kg/m^3	0.32
Specific heat ratio behind shock	1.35
Gas constant behind shock, J/kg · K	287
Static temp. behind shock, K	799

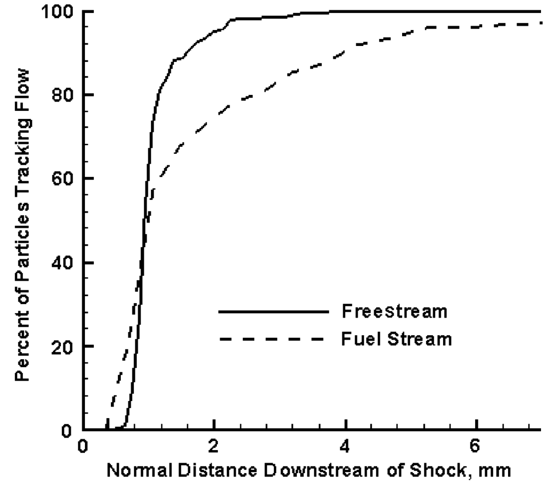

Fig. 11 Particle tracking behavior downstream of an oblique shock wave.

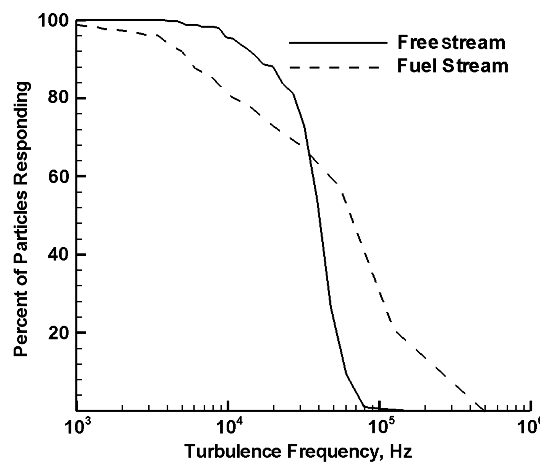

Fig. 12 Particle frequency response.

frequencies less than 10^4 Hz. The freestream particles are therefore more advantageous in terms of response to turbulence in the flow.

The reason for the success of the freestream particles in both cases is that the density of the silica powder is half that of the alumina powder. Despite approximately similar size distributions, the higher density gives the fuel stream particles more inertia, which has a negative impact on flow tracking across discontinuities and response to turbulence. These findings again pointed to the use of the silica powder in the fuel stream seeder for improved flow tracking performance in future PIV experiments.

Conclusions

Two unique particle seeders designed to seed the fuel stream and freestream of a scramjet for PIV measurements were presented. The goal of this work was to quantify the performance of these seeders in terms of particle size and shape. These results can be used to quantify the experimental uncertainty associated with these seeders with respect to flow tracking in future PIV measurements. The fuel stream seeder, using alumina powder, produced average particle sizes of 0.23 ± 0.03 and 0.49 ± 0.1 μm with helium and nitrogen as the seeding gases, respectively. The freestream seeder, using silica powder, produced an average particle size of 0.27 ± 0.07 μm. SEM images showed that the primary silica particles were nearly spherical, and the primary alumina particles were rounded, irregular, and ligamental. Based on these results, it was predicted that the silica particles would scatter light more uniformly and track the flow more faithfully during PIV measurements. It is recommended for future work that the particles from both seeders be used to measure a flow discontinuity so that the accuracy of this prediction can be fully quantified.

Both seeders operated as expected and produced particles near the target size of 0.3 μm. However, due to the spherical shape and smaller size distribution of the silica particles, the silica powder is recommended for particle generation in the application of PIV to high-speed flows. In the case of the fuel stream seeder, the silica powder provides a great opportunity for improvement in signal-to-noise ratio and flow tracking response in future measurements. Use of the same seeding material in both seeders will also eliminate bias in the results due to different light scattering or flow tracking properties from each seeder's particles.

Appendix: Technical Specification of Seeders

Fuel Stream Seeder

Notes:

1) All flowpaths are $1/4$ in. copper tubing with $1/4$ in. Swagelok® connectors unless noted.

2) All joints are $1/4$ in. brass Swagelok connector unless noted.

3) All bends are $1/4$ in. Swagelok 90 deg elbows unless noted.

4) All valves are $1/4$ in. brass unless noted.

Flowpath A

A 2050-mm-long tube leads to a 50-mm-radius, 90 deg bend and is followed by 500 mm to a 10-mm-radius, 90 deg bend. Next, 30 mm of tube leads to the shearing nozzle. There is 1200 mm of $3/8$ in. tube downstream of the nozzle connected to 100 mm of $3/8$ in. acrylic tube, which is followed by 700 mm of $3/8$ in. tube.

Flowpath B

A 450-mm-long tube leads to a 30-mm-radius, 90 deg bend. Next is an 1820-mm-long, 1-in.-diam stainless steel tube fluidizer, with a 35 mm plenum upstream of the porous plug. Finally, a 140-mm-long, $1/16$ in. stainless steel pickup tube with a 30-mm-radius, 90 deg bend leads to the shearing nozzle.

Flowpath C

A 150-mm-long tube leads to 90 deg bend, which is followed by a 500-mm-long tube leading to a $3/8$ in. T junction.

Freestream Seeder

Notes

1) All flowpaths are $3/8$ in. copper tubing with $3/8$ Swagelok connectors unless noted.

2) All joints are $3/8$ in. brass Swagelok connectors unless noted.

3) All bends are $3/8$ in. Swagelok 90 deg elbows unless noted.

4) All valves are $3/8$ in. brass unless noted.

Inlet line

A 1240-mm-long tube leads to a regulator, and then a 100-mm-long tube leads to T junction.

Flowpath A

A 260-mm-long tube leads to an elbow and is followed by a 4200-mm-long tube. This tube leads to an elbow, and then a 160-mm-long tube leads to a T junction. Finally, a 1250-mm-long tube leads to the outlet.

Flowpath B

A 1250-mm-long tube leads to an elbow and is followed by a 170-mm-long tube. This leads to a T junction, and then a 200-mm-long tube leads to the fluidizer. The fluidizer is 870 mm long, 110 mm in diameter, and has a 30 mm plenum upstream of the porous plug. Downstream of fluidizer, a 230-mm-long tube leads to a 30-mm-radius, 90 deg bend and is followed by a 320-mm-long tube going to T junction.

Acknowledgments

This work was sponsored by NASA with Glenn Diskin as technical monitor. The authors would also like to thank Kemit Finch, Josh King, and Dan Glanz for their work in designing and implementing the freestream seeder. Thanks also to Zach Owens for his sampling work on the fuel stream seeder and Bernadette Goncz for her work in examining the isokinetic nature of the fuel stream sampling experiments. Finally, the authors appreciate the assistance of Roland Krauss and Jim McDaniel.

References

[1] Goyne, C. P., Rodriguez, C. G., Krauss, R. H., McDaniel, J. C., and McClinton, C. R., "Experimental and Numerical Study of a Dual-Mode Scramjet Combustor," *Journal of Propulsion and Power*, Vol. 22, No. 3, May–June 2006, pp. 481–489.
doi:10.2514/1.13215

[2] Ahn, K., Kim, J. H., and Yoon, Y., "Application of PIV to Over-Expanded Supersonic Flows: Possibilities and Limits," *Journal of Visualization*, Vol. 6, No. 4, 2003, pp. 353–361.
doi:10.1007/BF03181742

[3] Melling, A., "Tracer Particles and Seeding for Particle Image Velocimetry," *Measurement Science and Technology*, Vol. 8, 1997, pp. 1406–1416.
doi:10.1088/0957-0233/8/12/005

[4] Meyers, J. F., *Generation of Particles and Seeding, Laser Velocimetry*, Lecture Series 1991–08, Von Karman Institute for Fluid Dynamics, Belgium, June 1991.

[5] Raffel, M., Willert, C. E., and Kompenhans, J., *Particle Image Velocimetry: A Practical Guide*, Springer–Verlag, Berlin, 1998.

[6] Krauss, R. H., McDaniel, J. C., Scott, J. E., Whitehurst, R. B., Segal, C., Mahoney, G. T., and Childers, J. M., "Unique, Clean-Air, Continuous-Flow, High-Stagnation-Temperature Facility for Supersonic Combustion Research," AIAA Paper 88-3059, July 1988.

[7] Krauss, R. H., and McDaniel, J. C., "A Clean Air Continuous Flow Propulsion Facility," AIAA Paper 92-3912, July 1992.

[8] Smith, C. T., and Goyne, C. P., "Three-Component Velocimetry in a Scramjet Combustor," AIAA Paper 2008-5073, July 2008.

[9] Samimy, M., and Lele, S. K., "Motion of Particles with Inertia in a Compressible Free Shear Layer," *Physics of Fluids*, Vol. 3, No. 8, Aug. 1991, pp. 1915–1923.
doi:10.1063/1.857921

[10] Goyne, C. P., McDaniel, J. C., Krauss, R. H., and Day, S. W., "Velocity Measurement in a Dual-Mode Supersonic Combustor Using Particle Image Velocimetry," AIAA Paper 2001-1761, April 2001.

[11] Ross, C. B., Lourenco, L. M., and Krothapolli, A., "Particle Image Velocimetry Measurements in a Shock-Containing Supersonic Flow," AIAA Paper 94-0047, Jan. 1994.

[12] Kadambi, J. R., Martin, W. T., Amirthaganesh, S., and Wernet, M. P., "Particle Sizing Using Particle Imaging Velocimetry for Two-Phase Flows," *Powder Technology*, Vol. 100, Nos. 2–3, Dec. 1998, pp. 251–259.
doi:10.1016/S0032-5910(98)00146-6

[13] Iacocca, R. G., and German, R. M., "A Comparison of Powder Particle Size Measuring Instruments," *International Journal of Powder Metallurgy*, Vol. 33, No. 8, 1997, pp. 35–48.

[14] Keane, R. D., and Adrian, R. J., "Optimization of Particle Image Velocimeters. Part I: Double Pulsed Systems," *Measurement Science and Technology*, Vol. 1, 1990, pp. 1202–1215.
doi:10.1088/0957-0233/1/11/013

[15] Smith, M. W., "Application of a Planar Doppler Velocimetry System to a High Reynolds Number Compressible Jet," AIAA Paper 98-0428, Jan. 1998.

[16] Goyne, C. P., McDaniel, J. C., Quagliaroli, T. M., Krauss, R. H., and Day, S. W., "Dual-Mode Combustion of Hydrogen in a Mach 5, Continuous-Flow Facility," *Journal of Propulsion and Power*, Vol. 17, No. 6, 2001, pp. 1313–1318.
doi:10.2514/2.5880

[17] Lide, D. R., and Frederikse, H. P. R. (eds.), *CRC Handbook of Chemistry and Physics*, 75th ed., CRC Press, Boca Raton, FL, 1994, pp. 4–95.

[18] Vallero, D. A., "Behavior of Particles at Sampling Inlets," *Fundamentals of Air Pollution*, Academic Press, New York/London/Orlando,

FL, 2007, pp. 464–466.

[19] Owens, Z. C., Goyne, C. P., Krauss, R. H., and McDaniel, J. C., "Assessment of Particle Seeder Performance via Direct Flowfield Sampling," AIAA Paper 2003-918, Jan. 2003.

[20] Goncz, B., "Experimental Validation of a Particle Sampling Technique," B. S. Thesis, Department of Mechanical and Aerospace Engineering, University of Virginia, Charlottesville, VA, 2005.

[21] Nelson, P. R., Coffin, M., and Copeland, K. A. F., "Important Continuous Distributions," *Introductory Statistics for Engineering Experimentation*, Academic Press, New York/London/Orlando, FL, 2003, pp. 106–129.

[22] Laufer, G., *Introduction to Optics and Lasers in Engineering*, Cambridge University Press, Cambridge, England, 1996, pp. 117–119.

C. Segal
Associate Editor